phys. stat. sol. (a) **114**, 739 (1989)

Subject classification: 78.60; S10.1

School of Mathematical and Physical Sciences, University of Sussex, Brighton[1])

Kinetic Analysis of the New Sensitization Effect in the TL of Silica Optical Fibres

By

Y. KIRSH[2]), J. E. TOWNSEND[3]), and P. D. TOWNSEND

The kinetic parameters of the thermoluminescence induced by X-irradiation in Ge-silica optical fibres doped with Nd, are investigated. Initially the emission spectrum consists mainly of a band near 400 nm. The combined effect of irradiation and heating generates a new band, near 520 nm. The kinetic analysis shows that besides the broad distribution of activation energies which is typical of the amorphous silica, several monoenergetic traps are active as well. The shallower trap can be linked to the well known "110 °C peak" of quartz. It is suggested that the recombination of electrons with O_2^- hole centres produce the 400 nm emission while the 520 nm band is associated with a Nd^{3+} hole centre. Ge^{4+} is assumed to be the dominant electron trap.

Nous avons calculé les paramètres cinétiques du thermoluminescence, produit par les rayons X dans les fibres optiques, du type germano-silicate où il entre du Nd. Au commencement le spectre d'émission était principalement une bande à 400 nm. Cependant, après irradiation et chauffage il y a une bande nouvelle près de 520 nm. Les analyses monstrent qu'en plus d'un range des énergies d'activation, qui sont typique du silice amorphe, il y a quelques autres pièges avec les énergies bien definies. Les pièges peu profondes sont liées au pic de "110 °C" de silice. Nous avons proposé que la lumière de 400 nm est produit par des électrons aux centres de O_2^-. L'émission à 520 nm est un résultat de Nd^{3+}. Le Ge^{4+} est le piège électronique plus important.

1. Introduction

In several materials, the sensitivity of thermoluminescence (TL), i.e. the response to a unit dose, has shown a remarkable increase following the combined treatment of irradiation and thermal annealing. This effect is referred to as the sensitization of TL, or the pre-dose effect. The effect was first discovered by Cameron in LiF [1]. Fleming [2] found it in quartz (crystalline SiO_2) which soon attracted other researchers [3 to 5] due to the applications of quartz in TL dating. Recently, a new sensitization effect was found in optical fibres based on silica (amorphous SiO_2) containing Ge and Nd [6]. Following X- or β-irradiation, the fibre exhibited a broad TL peak at about 175 °C. Initially the emission spectrum consisted mainly of a band near 400 nm. However, irradiation followed by heating above 320 °C generated a green emission band, the intensity of which was directly related to the irradiation history of the material. An obvious application of this effect is a rereadable radiation dosimeter. This dosimeter was found to function also at high temperature exposure, up to 400 °C [6].

In the present work the TL curves in the blue and the green are analyzed following X-irradiation and annealing. The kinetic parameters of the various TL peaks are evaluated by applying standard methods of analysis, namely — the initial rise tech-

[1]) Brighton BN1 9QH, Great Britain.

[2]) Permanent address: Everyman's University, 16 Klausner St., Tel Aviv 61392.

[3]) Present address: Department of Electronics and Computer Sciences, University of Southampton, S09 5NH, Great Britain.

nique, and a best-fit programme which seeks the parameters optimally describing the experimental TL curve. The purpose of this analysis is to investigate the relation between the blue and green emissions, and to check whether previously suggested models for the sensitization of quartz [3, 5] can be applied to this case.

2. Experimental

The samples were step-index optical fibres of a germano-silicate core (4 mol% GeO_2) containing 450 ppm Nd^{3+} and an estimated 2 ppm of OH^-. The fibres were kept in the vacuum and irradiated at RT by a tungsten target X-ray tube (operated at 30 kV, 15 mA) which provided 30 Gy/min. After the irradiation, the sample was heated at a rate of 20 K/min up to 450 °C. In the course of the heating, the TL spectrum was scanned in the range 300 to 800 nm, by a Bausch and Lomb grating monochromator coupled to a stepping motor. The readings were later corrected for the wavelength sensitivity of the monochromator and photomultiplier (EMI 9659QA) by a Superbrain microcomputer. The monochromator resolution was usually 10 nm.

3. Results

Curves a and b in Fig. 1 describe glow curves which were recorded at 400 nm (a) and 520 nm (b) in the first TL run of the sample which was X-irradiated for 40 min After the first run, the sample was again X-irradiated at RT for 40 min and the TL was recorded once more. Curves c and d in Fig. 1 show the TL intensity in the second run, at 400 nm (c) and at 520 nm (d). It can be seen that the blue component increased by 50% following the irradiation and heating, while the green one was enhanced by a factor of 4. This is shown even more clearly in Fig. 2, which depicts the emission spectrum of the TL at 130° in the first run (a) and in the second run (b).

The accumulated dose in all the irradiations save the last one is often referred to as pre-dose, while the dose of the last irradiation is called test dose. Thus, in curves a, b of Fig. 1 the pre-dose is 0 and the test dose is 1.2 kGy while in Fig. 1 c, d both equal 1.2 kGy. The green band grows faster than the blue one and at higher pre-doses it becomes the dominant feature in the emission spectrum.

In order to evaluate the activation energies, the "initial rise" method was applied to samples after a pre-dose of 1.2 kGy and a similar test dose. For the initial rise mea-

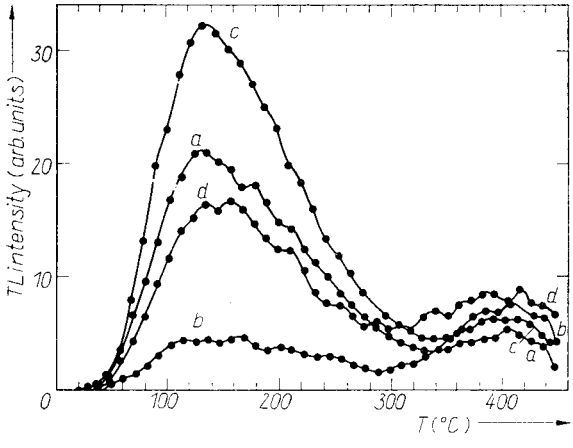

Fig. 1. Glow curves after X-irradiation. Curves a and b describe the TL in the first run at (a) 400 and (b) 520 nm. Curves c and d show the TL intensity in the second run, at (c) 400 and (d) 520 nm

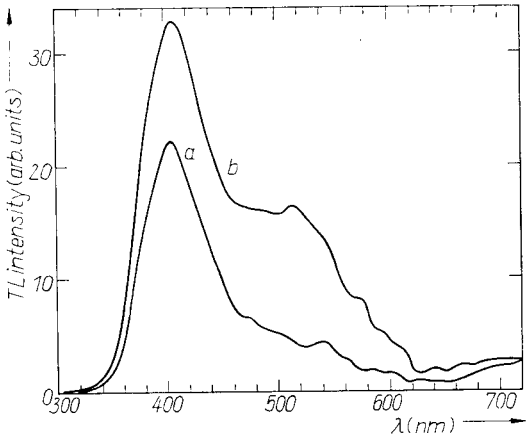

Fig. 2. TL emission spectra of the (a) first, and (b) the second runs; $T = 130$ °C

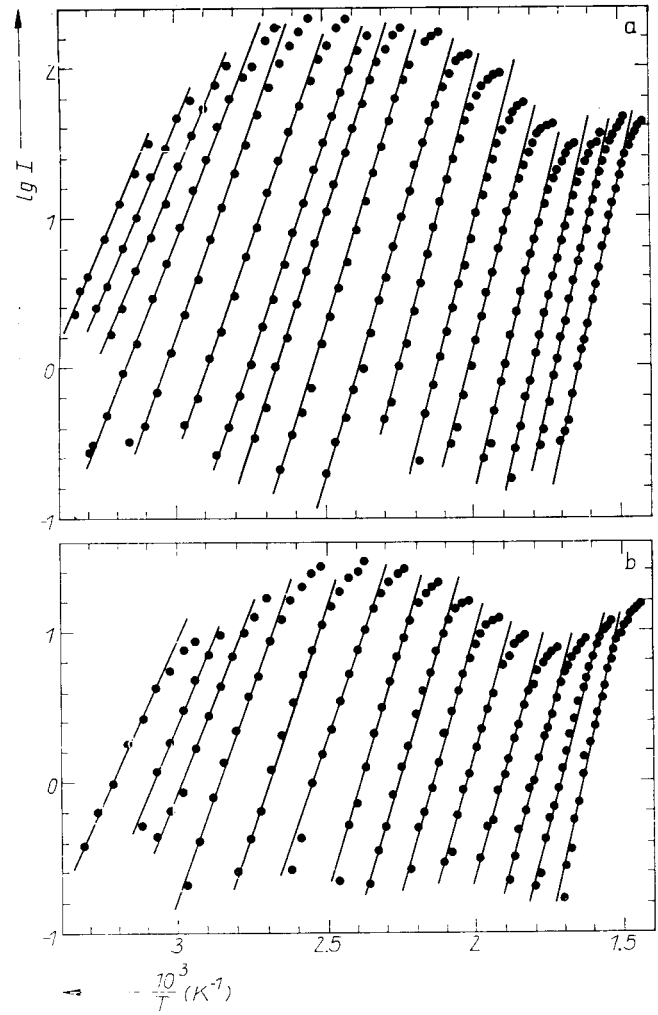

Fig. 3. Initial rise curves recorded at a) 400 and b) 520 nm

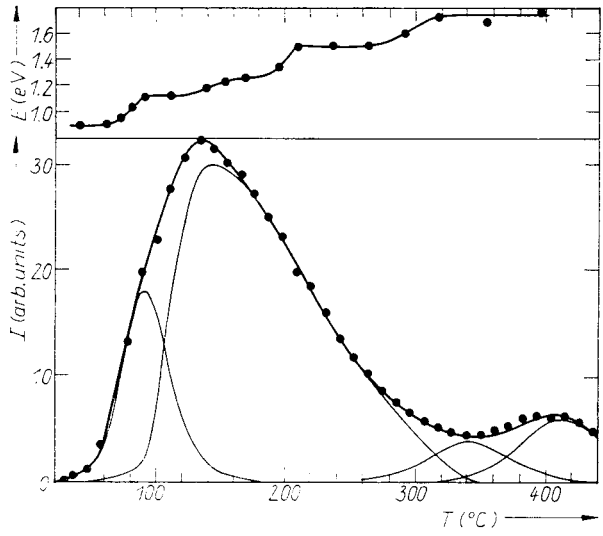

Fig. 4. Upper part: the dots represent the slope (E) and the centre of the linear part (T) of the curves in Fig. 3a. The resulting $E(T)$ curve is a stepwise function. Lower part: the best fit of the TL curve at 400 nm to the theoretical expressions. The experimental results are represented by dots. The curves represent the theoretical TL peaks, and their sum

surements the monochromator was set at a constant wavelength and the bandpass increased to 30 nm. Fig. 3 a and b show the initial rise curves recorded at 400 and 520 nm, respectively, by repetitive heating and cooling of the sample, each time reaching a higher temperature. When the natural logarithm of the intensity is plotted versus T^{-1} (K^{-1}), the slope of the linear part should be $-E/k$.

The activation energies E deduced from the slopes of the curves in Fig. 3a are represented by dots in the upper part of Fig. 4, where T is the temperature at the centre of the linear part. The resulting $E(T)$ curve is a stepwise function, indicating discrete traps with activation energies of 0.89, 1.49, and 1.72 eV. At the temperature range 90 to 200 °C the curve can be interpreted either as two discrete traps with $E_1 = 1.12$ eV, $E_2 = 1.26$ eV, or as a distribution of activation energies centred around 1.19 eV. It was shown by Rudlof et al. [7] that applying the initial-rise method to such a distribution results in a sloping step in the spectrum of activation energies, similar to the one which appears in the upper part of Fig. 4 near 150 °C.

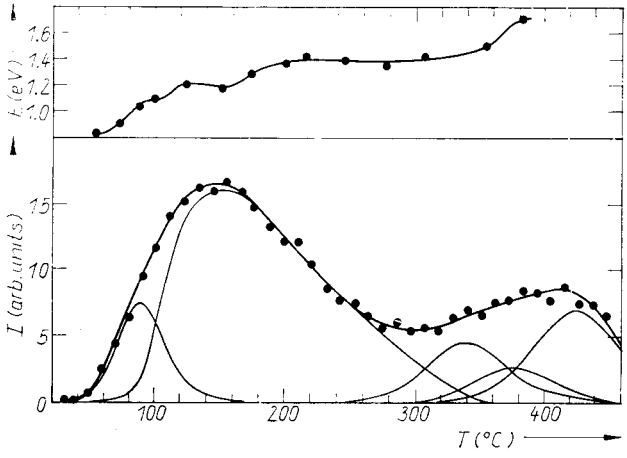

Fig. 5. The same as Fig. 4 for the TL curve at 520 nm

In the upper part of Fig. 5 the initial-rise spectrum is shown for the 520 nm TL curve. It indicates discrete activation energies of 0.83, 1.40, and 1.70 eV, while the 80 C° to 200 °C range can be interpreted either as two discrete traps of 1.08 and 1.20 eV, or as a distribution around 1.14 eV.

The values of E obtained by the initial-rise method were used as input in a best fit algorithm aimed at expressing the TL curve as the sum of individual peaks of general-order kinetics

$$I = -\frac{\mathrm{d}n}{\mathrm{d}t} = s' n^b \exp\left(-\frac{E}{kT}\right), \tag{1}$$

where I is the light intensity, n the concentration of not-yet-empty traps, and b the kinetic order. By integrating (1) an explicit expression for $I(T)$ can be evaluated, in which the parameters E, b, β (the heating rate), and s appear, where $s = s' n_0^{b-1}$ has the dimension of s^{-1}. Since the initial-rise method has yielded close activation energies for the blue and the green TL curves, we tried to express both of the curves by the same set of kinetic parameters.

The result of the best-fit procedure for the 400 nm TL curve is shown in the lower part of Fig. 4. It was found that the low temperature and high temperature parts of the glow curve, could be described as single second-order peaks with the activation energies shown in Table 1. The small discrepancy between experimental results and theoretical expressions around 375 °C, indicates the presence of another very small peak there. The remaining big asymmetric peak centred at 145 °C could not be expressed as the sum of single peaks but fitted very well a distribution of traps with a continuous spectrum of activation energies. Assuming a frequency-factor of the order of magnitude of the other peaks ($5 \times 10^{10}\ s^{-1}$) we found that the limits of the distribution are 0.94 and 1.35 eV. This is a broader distribution than indicated by the initial-rise, but one has to remember that due to overlapping with adjacent peaks, the low temperature and high temperature tails of the distribution cannot be analyzed by the initial-rise method.

In the lower part of Fig. 5 the result of the best-fit procedure is shown for the 520 nm curve. Here again the glow curve is nicely described as the sum of four single peaks and a broad distribution. The kinetic parameters appear in Table 2. The 375 °C peak is stronger here and its kinetic parameters can be evaluated. The scattering of the experimental dots around the theoretical curve is greater than for the 400 nm case (Fig. 4). This is explicable in signal-to-noise terms. The TL signal is stronger in 400 nm than in 520 nm, while the noise is getting higher with the increasing wavelength due to the changing sensitivity of the photomultiplier.

Table 1

Kinetic parameters of TL peaks in X-irradiated optical fibre recorded at 400 nm. E_{IR} is the activation energy according to the initial-rise method. E_{BF}, s, and b are the activation energy, frequency factor, and order of reaction, evaluated by a best-fit algorithm. The 145 °C peak is better described by a distribution of traps rather than by a single trap

peak	T (°C)	E_{IR} (eV)	E_{BF} (eV)	s ($10^{10}\ s^{-1}$)	b
1	91	0.89	0.86	1.9	2
2	145	1.12 to 1.26	0.94 to 1.35	5	2
3	340	1.49	1.45	1.2	2
4	375	—	—	—	—
5	412	1.72	1.72	6.0	2

Table 2
The kinetic parameters of the TL peaks recorded at 520 nm

peak	T (°C)	E_{TR} (eV)	E_{BF} (eV)	s (10^{10} s^{-1})	b
1	89	0.83	0.86	2.2	2
2	155	1.08 to 1.20	0.94 to 1.35	5	2
3	340	1.40	1.45	1.2	2
4	377	—	1.68	1.5	2
5	424	1.70	1.72	3.5	2

It should be emphasized that due to the high overlapping, the presentation of each curve as the sum of TL peaks is not unique. The E_{BF} and s values in Tables 1 and 2 are based on the presumption that the same set of traps is involved in both the blue and green emissions. However, slightly different parameters could provide an equally perfect fit. Similarly, the curves could be described as the sum of first-order peaks, although the fit would not be as good as with the second-order peaks.

4. Discussion

It was shown in this work that both the 400 and the 520 nm components of the TL could be described by the same set of activation energies (E_{BF} in Tables 1 and 2). One can therefore reach the conclusion that the blue and green bands involve the same system of traps, and that the enhancement of the green band following the irradiation and heating should be explained in terms of changes in the recombination centres rather than in the trap system. Taking into account the evidences that above RT all the TL peaks in SiO_2 involve electron traps and hole recombination centres [8 to 11] the following tentative model emerges. Initially, several electron traps and one hole centre are active between RT and 450 °C. The recombinations of thermally released electrons at the hole centre give rise to the band near 400 nm. The pre-dose and heating form another hole centre which causes the 520 nm band.

It should be remembered that due to the high overlapping, the presentation of the TL peaks by E_{BF} in Tables 1 and 2 is not unique. Taking into account the E_{TR} values, it seems that the activation energies of the green band are slightly lower than those of the blue band. These small differences might indicate that the traps and recombination centres are not totally independent. Close proximity of such pairs of defects may cause small perturbations of the activation energies.

The appearance of the new recombination centre might be accounted for by Zimmerman's model [3] which was suggested in order to explain the sensitization of the 110 °C peak in quartz. Basically, the model assumes two hole centres: L, which is the TL recombination centre, and a "hole reservoir" R, which is a shallower trap with a higher probability for capturing holes. During the pre-dose irradiation holes accumulate in R. Upon the subsequent heating they are thermally released to the valence band and trapped in L. Since more holes are now available in L, the sensitivity of the sample to a given test dose (which fills the electron traps) increases. Modifications to the model which were proposed by Chen [5] and David [12] have not changed its basic features. Attempts to correlate the traps and centres in the model with actual defects in natural and synthetic samples of quartz [12 to 16] have shown that the filling of L is often more complicated than the simple transfer process assumed by Zimmerman. For example, in samples containing OH^- and alkali ions the pre-dose effect was found to occur through the modification of oxygen hole centres rather than the

filling of existing traps [15, 16]. However, taking into account the bulk of the available data, one can say that Zimmerman's model provides a good phenomenological approximation to "real life" situations.

The defects involved in the sensitization of our samples are, of course, not necessarily the same as in natural quartz. Indeed, the intensity of the green band in our samples depends on the temperature of the thermal annealing according to an Arrhenius law, indicating that the transfer requires an activation energy of 0.52 eV [6]. The 110 °C peak in quartz was found to obey the same law with activation energies of 1.34 to 1.55 eV [17]. In addition, in order to adapt Zimmerman's model to our samples one has to assume two recombination centres, L_B and L_G, for the blue and green emissions, respectively. L_B can be filled during the irradiation while L_G is filled mainly during the heating stage, through the depletion of R.

The kinetic data indicate that besides the broad distribution of activation energies which is typical of the amorphous silica [11], several monoenergetic traps are active in our samples as well (see Tables 1, 2 and Fig. 4, 5). The first peak can apparently be identified with the well-known "110 °C peak" of quartz which actually occurs between 85 and 110 °C in a wide variety of SiO_2 samples [11, 18, 19]. Note that the reference to the 110 °C peak is normally made when using a high heating rate. In the present work the peak temperature corresponds to the 90 °C peak. The activation energy of 0.86 eV measured by us for this peak is in good agreement with previous reports [18, 19]. The peak has been ascribed to a complex defect with Al and OH impurities, which explains why it is quite intense in natural SiO_2, but rather small in highly pure synthetic samples [6]. The peaks near 340 and 375 °C are probably related to traps which act as "donors" in phototransfer experiments and which usually give TL peaks at $\approx$ 325 and 375 °C [11].

A comment is due here concerning the order of the kinetics. In crystalline quartz all the TL peaks appear to be of first order [19 to 21]. It might indicate a close proximity of traps and recombination centres which leads to negligible retrapping. In silica, on the other hand, second-order kinetics seem to prevail [21, 22]. Our results favour the second order, but one cannot tell whether it is a "genuine" bimolecular process due to strong retrapping, or a "spurious" one due to traps having a narrow distribution of activation energies, each releasing electrons monomolecularly.

Since our samples are formed as highly pure glass matrix with well controlled dopant levels, any attempt to identify the traps and centres should consider Ge and Nd ions as the main extrinsic defects. Ge is tetravalent, like Si, and it substitutes Si in the SiO_2 lattice. However, its higher electron affinity makes it an efficient electron trap, with or without charge compensator [14]. Its high content in our fibres (4 mol%) suggests that Ge in various environments (to account for the distribution of activation energies) plays an important role in the TL process, as a high concentration electron trap. As for Nd, its valence is usually +3 and it should form a hole trap if it enters the lattice substitutionally for Si. Indeed, in natural quartz Al^{3+} is an important hole trap [11, 23] and one can expect Nd^{3+} to behave similarly.

Several intrinsic defects may also play a role in the TL. Oxygen vacancies (E′ centres) act as electron traps. They appear in quartz only after particle irradiation but have been observed in as-grown silica [24, 25]. Oxygen interstitials as well as O_2^{2-} molecular ions (a pair of a lattice oxygen and an interstitional one) can act as hole traps [24 to 27]. Broken Si–O bonds are readily created by ionizing radiation and are also presented in as-grown material, especially silica [28 to 31]. The resulting dangling oxygen bonds and empty Si orbitals are potential hole and electron traps, respectively.

In order to evaluate the relative importance of the various hole centres in the TL process, reliable information on the origin of the 400 and 520 nm bands would have

been very useful. Unfortunately, the relevant literature suggests several conflicting models for the origin of the blue emission, and almost no reference to the green one. Recently, however, it was shown [26] that the blue emission of silica actually contains three bands, near 295, 400, and 460 nm (4.2, 3.1, and 2.7 eV) and that there is strong experimental evidence which relates the 400 nm band to O_2^- molecular ion (O_2^{-2} which trapped a hole). This model is in agreement with measurements in our laboratory [6] in which the 400 nm band was found to be the major feature in the TL and radioluminescence of a wide variety of doped and undoped silica fibres, indicating that the luminescent centre is an intrinsic defect.

As for the green band, the reference in the literature is scarce, but since only Nd-doped fibres were found to exhibit this band in preliminary experiments [6], its origin is probably a hole recombination centre in which a Nd^{3+} ion is incorporated. It should be noted that in the recombination of electrons with Al^{3+}-h^+ centres, a similar band is produced at 470 nm [14].

To conclude, we suggest the following tentative model for the sensitization of TL in Ge-silica:Nd^{3+} fibres. Initially, the main radiative process during the heating of the irradiated sample is the recombination of thermally released electrons with O_2^- hole centres, to produce the 400 nm emission. Thermal annealing of the irradiated sample introduces another hole centre which probably involves the Nd^{3+} ion. The recombination of an electron with this centre produces the 520 nm band. Ge^{4+} might be the dominant electron trap in both cases.

In terms of the "extended Zimmerman's model" L_B is the O_2^{2-} hole trap while L_G is a hole trap which involves the Nd^{3+} ion. If the filling of L_G requires only the transfer of holes from the reservoir R, then R is probably a common intrinsic defect such as a broken oxygen bond. However, in this instance it may be appropriate to consider changes in the concentration of defect sites rather than in the electronic population. The accumulative growth of the green band, which is linear both in the pre-dose and in the test dose, is compatible with the production of a new defect complex. It might involve the migration of an ionic defect which becomes mobile above 320 °C.

References

[1] J. R. CAMERON, Health Phys. **10**, 25 (1964).
[2] S. J. FLEMING, Thermoluminescence of Geological Materials, Ed. D. J. MCDOUGALL, Academic Press, New York 1968 (p. 431).
[3] J. ZIMMERMAN, J. Phys. C **4**, 3265 (1971).
[4] M. J. AITKEN, Counc. Eur. PACT J. **3**, 319 (1979).
[5] R. CHEN, Counc. Eur. PACT J. **3**, 325 (1979).
[6] A. D. ELLIS, P. D. MOSKOWITZ, J. E. TOWNSEND, and P. D. TOWNSEND, J. Phys., to be published.
[7] G. RUDLOF, J. BECHERER, and H. GLAEFEKE, phys. stat. sol. (a) **49**, K121 (1978).
[8] M. SCHLESINGER, J. Phys. Chem. Solids **26**, 1761 (1965).
[9] I. K. BAILIFF, S. G. E. BOWMAN, S. F. MOBBS, and M. J. AITKEN, J. Electrostat. **3**, 269 (1977).
[10] S. G. E. BOWMAN, Counc. Eur. PACT J. **3**, 381 (1979).
[11] S. W. S. MCKEEVER, Radiat. Protect Dosimetry **8**, 81 (1984).
[12] M. DAVID, Indian J. pure appl. Phys. **19**, 1048 (1981).
[13] M. BOHM, W. PESCHKE, and A. SCHARMANN, Radiat. Eff. **53**, 67 (1980).
[14] S. W. S. MCKEEVER, C. Y. CHEN, and L. E. HALLIBURTON, Nuclear Tracks **10**, 489 (1985).
[15] M. MARTINI, E. SIBILIA, G. SPINOLO, and A. VEDDA, Nuclear Tracks **10**, 497 (1985).
[16] M. MARTINI, G. SPINOLO, and A. VEDDA, J. appl. Phys. **61**, 2486 (1987).
[17] S. J. FLEMING, Thermoluminescence Techniques in Archaeology, Clarendon Press, Oxford 1979 (p. 125).

[18] A. Delunas, V. Maxia, and G. Spano, Lettere Nuovo Cimento **36**, 44 (1983).
[19] M. David, S. P. Kathuria, and C. M. Sunta, Indian J. pure appl. Phys. **20**, 519 (1982).
[20] P. W. Levy, Counc. Eur. PACT J. **3**, 466 (1979).
[21] P. L. Mattern, K. Lengweiler, and P. W. Levy, Radiat. Eff. **26**, 237 (1975).
[22] R. H. West and A. C. Carter, Radiat. Eff. Letters **57**, 129 (1980).
[23] S. A. Durrani, K. A. R. Khazal, S. W. S. McKeever, and R. J. Riley, Radiat. Eff. **33**, 237 (1977).
[24] P. W. Levy, J. Phys. Chem. Solids **13**, 287 (1960).
[25] C. M. Nelson and J. H. Crawford, J. Phys. Chem. Solids **13**, 295 (1960).
[26] M. Guzzi, M. Martini, M. Mattaini, F. Pio, and G. Spinolo, Phys. Rev. B **35**, 9407 (1987).
[27] M. Martini, G. Spinolo, and A. Vedda, J. Lum. **40/41**, 347 (1988).
[28] M. Stapelbroek, D. L. Griscom, E. J. Friebele, and G. H. Sigel, J. non-crystall. Solids **32**, 313 (1976).
[29] G. N. Greaves, Phil. Mag. **B37**, 447 (1978).
[30] G. Lucovsky, Phil. Mag. **B39**, 513, 531 (1979).
[31] G. Lucovsky, J. non-crystall. Solids **35/36**, 825 (1980).

(Received August 22, 1988)